



Voltage Regulation Using a Permanent Magnet Synchronous Generator with a Series Compensator

Preprint

P. Hsu,¹ Z. Wu,² E. Muljadi,³ and W. Gao²

¹ *San Jose State University*

² *University of Denver*

³ *National Renewable Energy Laboratory*

*To be presented at the IEEE Energy Conversion Congress and
Exposition*

Montreal, Canada

September 20–24, 2015

**NREL is a national laboratory of the U.S. Department of Energy
Office of Energy Efficiency & Renewable Energy
Operated by the Alliance for Sustainable Energy, LLC**

This report is available at no cost from the National Renewable Energy
Laboratory (NREL) at www.nrel.gov/publications.

Conference Paper
NREL/CP-5D00-64747
August 2015

Contract No. DE-AC36-08GO28308

NOTICE

The submitted manuscript has been offered by an employee of the Alliance for Sustainable Energy, LLC (Alliance), a contractor of the US Government under Contract No. DE-AC36-08GO28308. Accordingly, the US Government and Alliance retain a nonexclusive royalty-free license to publish or reproduce the published form of this contribution, or allow others to do so, for US Government purposes.

This report was prepared as an account of work sponsored by an agency of the United States government. Neither the United States government nor any agency thereof, nor any of their employees, makes any warranty, express or implied, or assumes any legal liability or responsibility for the accuracy, completeness, or usefulness of any information, apparatus, product, or process disclosed, or represents that its use would not infringe privately owned rights. Reference herein to any specific commercial product, process, or service by trade name, trademark, manufacturer, or otherwise does not necessarily constitute or imply its endorsement, recommendation, or favoring by the United States government or any agency thereof. The views and opinions of authors expressed herein do not necessarily state or reflect those of the United States government or any agency thereof.

This report is available at no cost from the National Renewable Energy Laboratory (NREL) at www.nrel.gov/publications.

Available electronically at SciTech Connect <http://www.osti.gov/scitech>

Available for a processing fee to U.S. Department of Energy and its contractors, in paper, from:

U.S. Department of Energy
Office of Scientific and Technical Information
P.O. Box 62
Oak Ridge, TN 37831-0062
OSTI <http://www.osti.gov>
Phone: 865.576.8401
Fax: 865.576.5728
Email: reports@osti.gov

Available for sale to the public, in paper, from:

U.S. Department of Commerce
National Technical Information Service
5301 Shawnee Road
Alexandria, VA 22312
NTIS <http://www.ntis.gov>
Phone: 800.553.6847 or 703.605.6000
Fax: 703.605.6900
Email: orders@ntis.gov

Cover Photos by Dennis Schroeder: (left to right) NREL 26173, NREL 18302, NREL 19758, NREL 29642, NREL 19795.

NREL prints on paper that contains recycled content.

Voltage Regulation Using a Permanent Magnet Synchronous Condenser with a Series Compensator

Ping Hsu
San Jose State Univ.
San Jose, CA

Ziping Wu
Univ. of Denver
Denver, CO

Eduard Muljadi
National Renewable Energy Lab
Golden, CO

Wenzhong Gao
Univ. of Denver
Denver, CO

Abstract — Wind power plant (WPP) is often operated at unity power factor, and the utility host where the WPP connected prefers to regulate the voltage. While this may not be an issue in a stiff grid, the connection to a weak grid can be a problematic. This paper explores the advantages of having voltage regulation capability via reactive power control. Another issue in wind power generation is that not all turbines are able to control its reactive power due to technical reason or contractual obligations. A synchronous condenser (SC) using a permanent magnet synchronous generator (PMSG) is proposed for providing necessary reactive power for regulating voltage at a weak grid connection. A PMSG has the advantage of higher efficiency and reliability. Because of its lack of a field winding, a PMSG is typically controlled by a full-power converter, which can be costly. In the proposed system, the reactive power of the SC is controlled by a serially connected compensator operating in a closed-loop configuration. The compensator also damps the PMSG's tendency to oscillate. The compensator's VA rating is only a fraction of the rating of the SC and the PMSG. In this initial investigation, the proposed scheme is shown to be effective by computer simulations.

Index Terms—Synchronous condenser, permanent magnet synchronous machine, reactive power control, voltage stabilization.

I. INTRODUCTION

High impedance of a weak grid connection limits the power transmission. In addition, some wind turbine generator (WTG) can only be operated at a unity power factor under different circumstances (e.g. contractual obligation). And in some other cases, the utility host where the wind power plant (WPP) is connected to, does not allow the WPP to control it is voltage at the point of interconnection (POI). In this paper, we will show the difference between the operation at unity power factor and the operation with a voltage control.

Voltage control requires the source of adjustable reactive power. With the assumption that the WTG can only be operated at unity power factor, we use synchronous condenser at the POI. Synchronous condensers (SCs) have been used traditionally in the power industry to support weak grids that have poor voltage regulation. Static equipment such as static synchronous compensators (STATCOMs) and static VAR compensators (SVCs) [1] are now often used for reactive power production. SVCs and STATCOMs have the advantage of faster responses [2]. Under certain grid fault conditions [3], SCs provide higher reactive power, and, more importantly, the kinetic energy stored in the rotor provides inertial support to the grid during faults [4]. The inertia support capability and

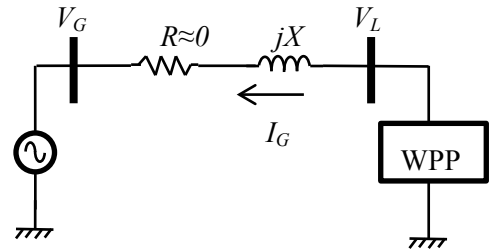
fast response time become more important as the grid-connection requirements (such as low-voltage ride-through and inertial response) for distributed generation become more stringent.

The proposed voltage regulation scheme is based on VAR compensation using a PMSG-based SC (PMSC) instead of a wound-field machine as in a traditional SC. The control of VAR output from the proposed SC is achieved by a series compensator connected to the PMSG. This compensator also damps the PMSG's tendency to oscillate when connected to an AC source [5]. A crowbar circuit should be used to protect the power electronics of the compensator circuit during a grid fault.

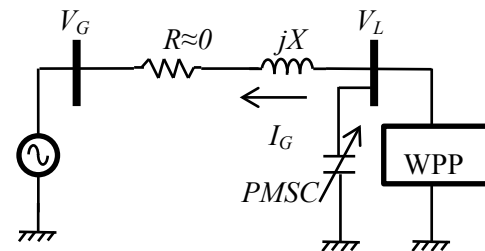
II. REACTIVE POWER CONTROL ADVANTAGE

2.1 Power Transmission Limitation

Fig. 1 shows a model of a wind power plant (WPP) connected to a weak grid. V_G and V_L in the figure represent the voltage at the infinite bus and at the point of interconnection (POI) of the WPP, respectively. R and jX represent the transmission line impedance. Note that in most cases the transmission line resistance is often considered negligible. In weak grids, the impedance is often five to ten times higher than stiff grids.



(a) WPP operate at unity power factor



(b) WPP operate at unity power factor with PMSC in parallel

Fig. 1. A wind power plant connected to a weak grid.

The current I_G in Fig. 1 can be expressed as in (1).

$$I_G = \frac{V_L - V_G}{jX} \quad (1)$$

The WPP output power is given in (2).

$$P = \frac{3V_L V_G}{X} \sin(\delta) \quad (2a)$$

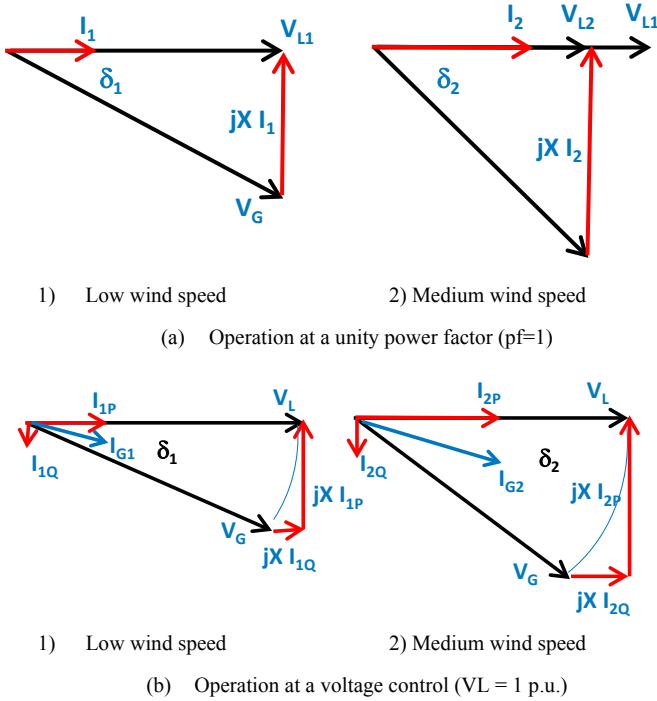


Fig. 2. Phasor diagram of WPP operated in two operating modes

From Figure 2, it is shown that as the power increases, the operation at unity power factor will produce a lower terminal voltage than operation at low wind speed ($V_{L2} < V_{L1}$). This voltage reduction will degrade the power transmission capability of the transmission line as shown in equation (2a).

In fact the voltage V_L depends on the phase angle δ and infinite bus voltage V_G ($V_L = V_G \cos \delta$). The power equation (2a) can be simplified for unity power factor operation by substituting the voltage V_G .

$$P = \frac{3V_G^2}{2X} \sin(2\delta) \quad (2b)$$

The power transmission capability for unity power factor operation, as shown in equation 2b, has a peak value 50% of the original equation 2a and it peaks at 45 degrees as compares to 90 degrees in the equation 2a. This limitation is even worse for a weak grid (large transmission reactance, X)

In contrast, the phasor diagram of the WPP operating by voltage control is shown in Figure 2b. It's clear that the power transmission is directly related to the phase angle δ between the grid voltage (V_G) and the output voltage of the WPP (V_L). From Figure 2b, it is clear that the voltage at the POI of the WPP is controllable by adjusting the output reactive power of

the PMSC, which is proportional to the reactive current I_Q . As shown in the phasor diagram in Figure 2b, increasing I_Q will increase voltage drop $jX I_Q$, which in effect adjusting the voltage V_L .

Thus, by controlling the V_L constant, through PMSC, we can maintain the maximum power transfer capability shown in equation (2a) constant. Figure 3 shows the power transmission capability curves for two cases (i): WPP operating at unity power factor and (ii) WPP is operating by controlling $V_L = 1$ by using the PMSC. As shown in the figure 3, power transmission capability can be maintained. This is accomplished by controlling the PMSC in parallel with the WPP to maintain the voltage at the WPP point of interconnection (POI), V_L , constant at rated value.

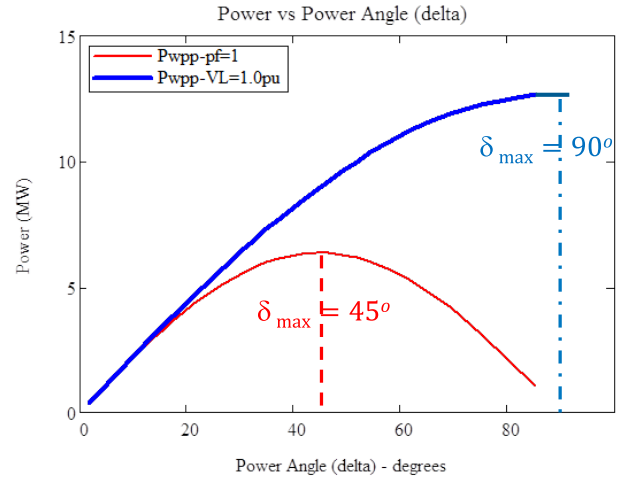


Fig. 3. Transmission Power vs. power angle

2.2 Reactive Power Control Implementation

Fig. 4 shows the configuration of the proposed PMSG-based SC. As shown, the controller's output voltage is connected in series to the phase windings of the PMSG through transformers. It is possible to directly connect the compensator output in series to the PMSG (without the transformers) if the inverter circuit in the compensator is properly designed.

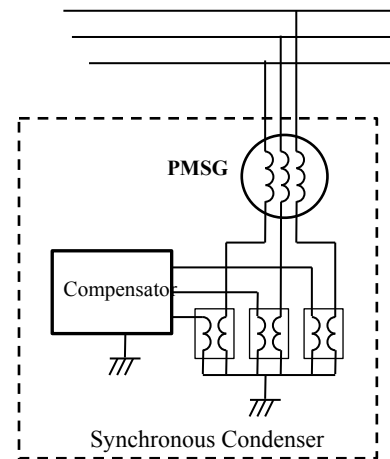


Fig. 4. Configuration of the proposed synchronous condenser.

The connection can also be made on the grid side if the common point of the PMSG's Y-connection cannot be accessed and separated. In this case, the direct connection to the compensator inverter circuit would be of the high voltage and lack of a common voltage reference point.

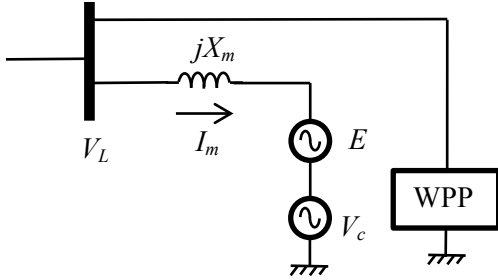


Fig. 5. Equivalent circuit of the configuration shown in Fig. 1.

Fig. 5 shows the equivalent circuit of the SC with the series compensator, where V_c represents the compensator output voltage, E represents the voltage from the internal emf of the PMSG, and X_m is the PMSG's impedance.

The compensator output voltage, V_c , is controlled to be in-phase with V_L via a phase-locked loop. Also, the PMSG has no mechanical loading. Under such conditions, all three voltages— V_L , V_c , and E —are in phase. In this case, if V_c is positively in phase with E and $|V_c|$ is high enough such that $V_c + E > V_L$, the effect is the same as a synchronous wound-field machine that is overexcited and provides VAR to the grid. If, on the other hand, V_c is 180 degrees out of phase with E and $|V_c|$ is high enough such that $V_c + E < V_L$, the effect is the same as a synchronous machine that is underexcited and absorbs VAR from the grid. This operation is described by equation (3) and (4) below. The current I_m in this circuit is given by (3), and the complex power drawn by the SC is given in (4), where the superscript asterisk represents complex-conjugate operation.

$$I_m = \frac{V_L - (E + V_c)}{jX_m} \quad (3)$$

$$S = V_L \cdot I_m^* = V_L \left(\frac{V_L - (E + V_c)}{jX_m} \right)^* \quad (4)$$

Under the condition that all three voltages— V_L , V_c , and E —are in phase, the complex power, S , given by (4) is pure imaginary. In other words, this subsystem only produces or consumes VARs and the amount of VARs can be controlled by the signed magnitude of the compensator output voltage, V_c .

In normal operating conditions, the value of E in (4) remains nearly constant, because the PMSG's speed only slightly fluctuates about the synchronous speed, and E , by design, matches the nominal voltage of V_L . Under this condition, the compensator output, V_c , can be varied to produce the necessary reactive power to support a WPP for a weak grid connection.

2.3 Damping Control

Equation (5) is the control law for damping the PMSG's tendency of oscillation when directly connected to the grid [5]. The following nomenclatures are used in (5).

- L_m : PMSG inductance
- R_m : Resistance of the stator windings
- v_{qc}, v_{dc} : q and d axis voltage of the compensator [6]
- ω, ω_{sync} : generator mechanical speed and sync speed
- ε : a small number for the pseudo-differentiator
- k_b : damping constant

$$\begin{bmatrix} v_{dc}(s) \\ v_{qc}(s) \end{bmatrix} = \begin{bmatrix} -\omega L_m \\ \frac{L_m s}{\varepsilon s + 1} + R_m \end{bmatrix} k_b (\omega_{sync} - \omega) \quad (5)$$

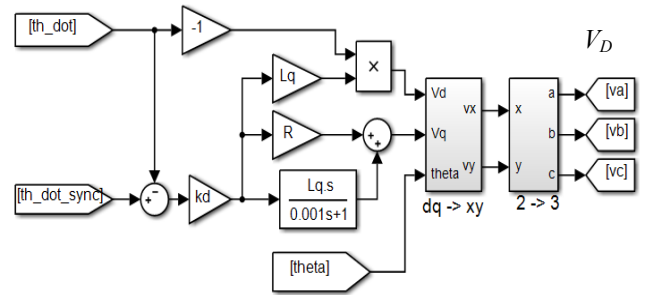


Fig. 6. The damping control implementation diagram.

The implementation of the damping control law (5) requires two additional transformation operations: a transformation from a dq frame to a synchronous frame and a transformation from two-phase to three-phase, as shown in Fig. 6 [5]. V_D in Fig.6 is the result from these transformations. V_D and a reactive power control voltage (described in the following section) constitute the compensator output voltage.

III. VAR COMPENSATION CONTROLLER

The main objective of the compensator is to control the production of reactive power that is necessary to maintain the voltage V_L at the nominal value. This is done by controlling the compensator output, V_c , according to the PI controller in (6). The phase of V_c is locked to the phase of V_L . The secondary control objective is to produce the damping effect to damp the oscillation of the PMSG, as explained earlier.

$$V_c = \left(k_p + \frac{k_i}{s} \right) (V_{ref} - |V_L|) \quad (6)$$

The output voltage of the compensator (V_{CMP}) is the sum of the voltage V_c and the damping control output V_D , as given in (5) and in Fig. 6. Fig. 7 is a functional block diagram of the overall voltage stabilizing control system. This block diagram includes an infinite bus of voltage V_G , transmission line dynamics (R and jX), WPP, and the SC (i.e., the PMSG) with the series compensator. The diagram also includes the structure of the damping control and the VAR control algorithm. V_{ref} in the figure is the reference voltage for the

WPP voltage control. A phase-locked loop is used to synchronize the phase of the WPP connection voltage and that of the compensator output voltage.

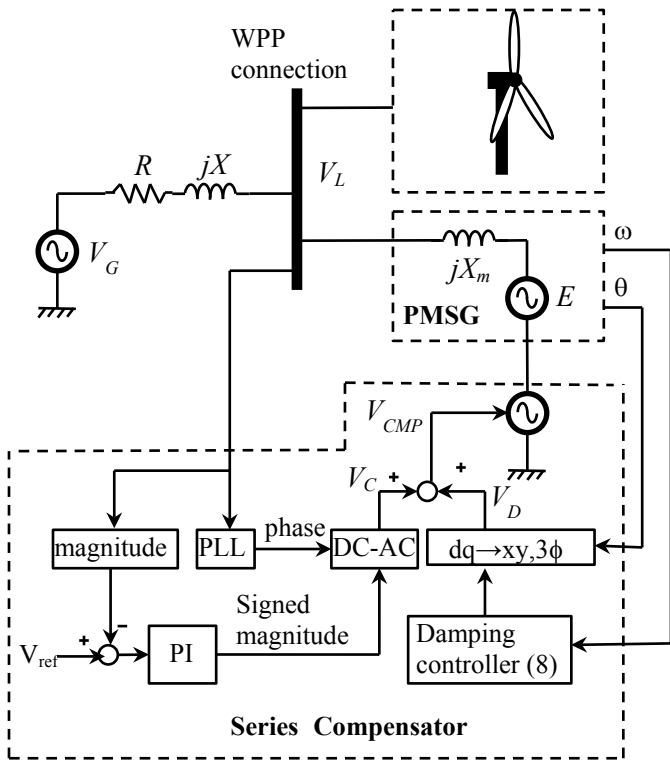


Fig. 7. A block diagram of the overall system.

IV. SIMULATION RESULTS

The computer simulation model is created based on the block diagram shown in Fig. 7. Following are the values of some of the key parameters used in the simulation.

- Line voltage: 12 kV
- Transmission line resistance: 0.01 Ω .
- Transmission line inductance: 30 mH
- PMSG inductance: 4 mH
- PMSG resistance: 0.05 Ω

Results from several simulation runs are shown in this section. In all the simulation runs, the power from the WPP is initially set to 0, and at 3 s it is ramped up to 10 MW (p.f. = 1 at 12 kv) in 2 s. At $t = 10$ s, the power is ramped back down to 0 in 2 s. As explained earlier, the output power from the WPP can be restricted by the transmission line if the grid is weak (X is large). Between 5 s and 10 s, the WPP attempts to deliver 10 MW, but this is not achieved in some of the simulation runs. Fig. 8 shows the results from the first simulation run, in which the proposed SC is not used. The transmission line inductance is set to 30 mH. The first and the second traces in this figure are the power and reactive power drawn from the infinite bus. The third trace is the voltage at the WPP connection, i.e., the RMS value of phase-to-phase voltage of V_L . As shown, as the output of the power is injected into the WPP connection, the voltage drops. In this case, the power only reached about 6 MW. The voltage at the WPP connection drops to about 7kV.

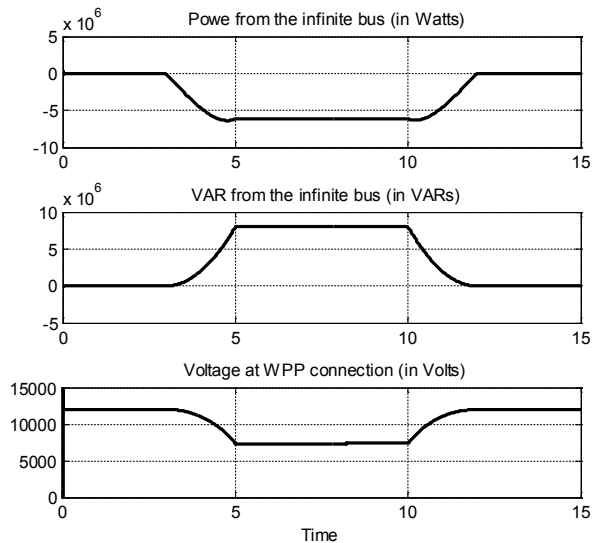


Fig. 8. Results from Simulation #1 (no SC is used): power from the infinite bus, VAR from the finite bus, and the voltage at the WPP POI.

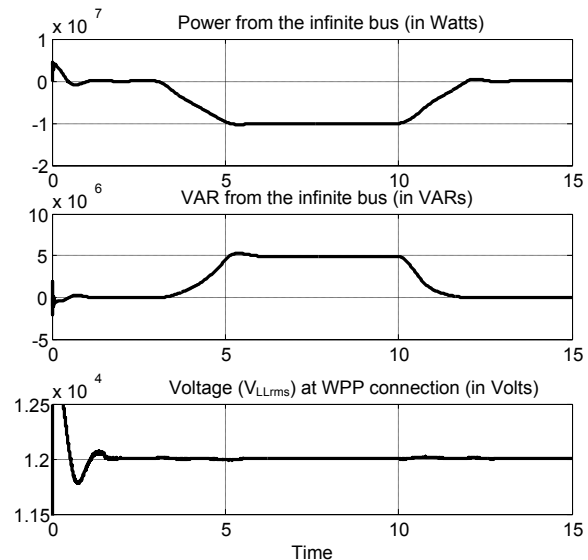


Fig. 9. Results from Simulation run #2 (SC is used): power from the infinite bus, VAR from the infinite bus, and the voltage at the WPP connection.

Fig. 9 and Fig. 10 show simulation results from the second run, which has the same condition as the first except that the proposed SC is used. Traces in Fig. 9 correspond to those in Fig. 8. Fig. 9 shows that, with the SC, the output power from the WPP can reach 10 MW and the operation is stable. As shown by the third trace, the voltage at the WPP connection is kept nearly constant at the nominal value. The initial transient is due to the initial condition of the simulation model. The traces shown in Fig. 10 are the power and VAR delivered to the SC and the compensator output voltage, and the PMSG phase voltage. These traces are generated from the same simulation run as that shown in Fig. 9. The first trace in Fig. 10 shows that SC does not deliver or consume real power. The second trace shows that the SC provides approximately 5 MVar reactive power to the WPP connection. This amount is the same as the reactive power provided by the infinite bus. The third trace is the output voltage from the compensator

(V_{CMP} in Fig. 7). As shown, the peak value is approximately 1 kV, which is about only 10% of the phase voltage of the system. This shows that the VA rating of the compensator is approximately 10% of the rating of the SC. The last trace in Fig. 10 shows the PMSG's phase voltage. This voltage is lower than the nominal value because of the voltage across the compensator.

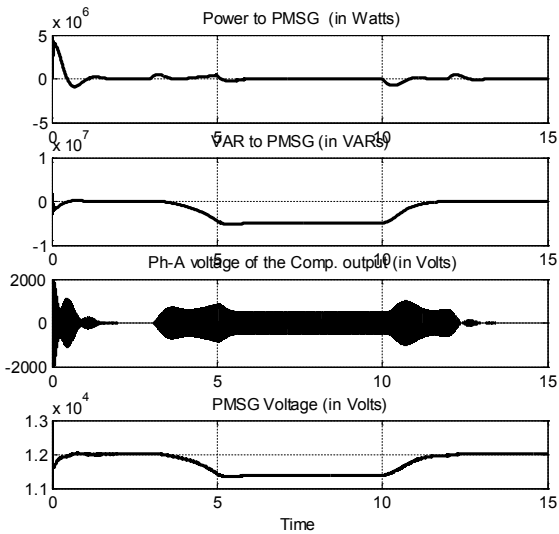


Fig. 10. Results from Simulation #2 (SC is used): power to the PMSG, VAR to the PMSG, phase-A output voltage of the compensator, and the line voltage of the PMSG.

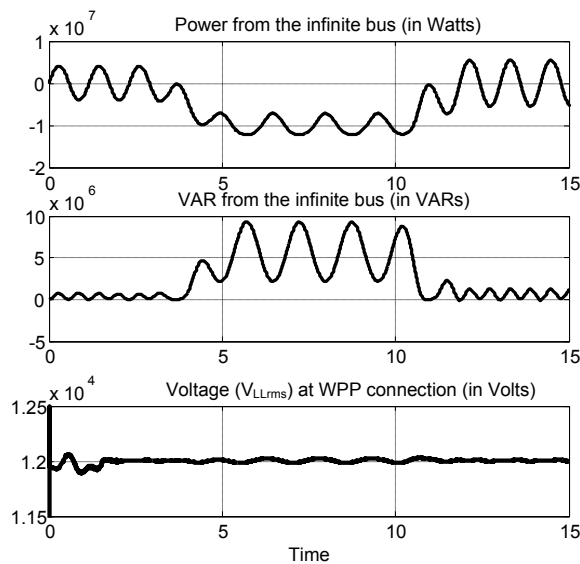


Fig. 11. All traces correspond to those in Fig. 8. In this simulation, the damping control function of the compensator is disabled.

To demonstrate the effectiveness of the damping control, in the third simulation run, the damping control portion of the SC is disabled. The result of this simulation is shown in Fig. 11, where the traces correspond to those in Fig. 8. As shown, the system oscillates at a sub-synchronous frequency. This is because of the lack of mechanical damping and the interaction between the PMSG rotor inertia and the electromagnetic torque as affected to the load angle.

V. CONCLUSION

In this paper, we illustrate the benefit of voltage controllability of a wind power plant. We propose using a PMSG instead of a wound-field machine for SCs to regular the voltage at the point of connection.

A PMSC has the advantage over a STATCOM or SVC from being able to provide real power in a frequency drop condition (provided by the rotating mass—inertial response). The voltage regulation is achieved by controlling reactive power using a serially connected inverter in the proposed PMSC. This serially connected converter can react to the grid condition faster than that of a wound-field machine and its VA rating is only a fraction of the rating of the SC. The proposed scheme is demonstrated in a system model where a wind power plant is connected to a weak grid. The proposed scheme is shown to be effective based on the preliminary study we have performed.

VI. ACKNOWLEDGMENT

This work was supported by the U.S. Department of Energy under Contract No. DE-AC36-08-GO28308 with the National Renewable Energy Laboratory and by the San Jose State University, San Jose, California.

VII. REFERENCES

- [1] H. A. Kojori, S. B. Dewan and J. D. Lavers, "A large-scale PWM solid-state synchronous condenser," *IEEE Transactions on Industry Applications*, vol. 28, no. 1, 1992.
- [2] M. F. Soheil Ganjefar, "Comparing SVC and synchronous condenser performance in mitigating torsional oscillations," *International Transactions on Electrical Energy Systems*, vol. Wiley Online Library, 2014.
- [3] S. Teleke, T. Abdulahovic, T. Thiringer and J. Svensson, "Dynamic performance comparison of synchronous condenser and SVC," *IEEE Transactions on Power Delivery*, vol. 23, no. 3, 2008.
- [4] N. Mendis, k. Muttaqi and S. Perera, "Management of battery-supercapacitor hybrid energy storage and synchronous condenser for isolated operation of PMSG-based variable-speed wind turbine generating systems," *IEEE Transaction on Smart Grid*, vol. 5, no. 2, pp. 944-953, 2014.
- [5] P. Hsu and E. Muljadi, "Damping control for permanent magnet synchronous generators and its application in a multi-turbine system." in *Australasian Universities Power Engineering Conference, AUPEC*, 2014.
- [6] D. Novotny and T. Lipo, *Vectro Control and Dynamics of AC Drives*, Oxford, 1997.

VIII. BIOGRAPHIES



Ping Hsu (M'1990) graduated from the University of California at Berkeley in 1988 with a Ph.D. in electrical engineering. He joined the Department of Mechanical and Industrial Engineering at the University of Illinois at Urbana-Champaign in 1989, and in 1990 he joined the Department of Electrical Engineering at San Jose State University. At San Jose State University, he served as the associate dean of the College of Engineering from 2001 to 2007 and interim dean from 2012 to 2013. His research interests include control theory, robotics, power electronics, machine control, and renewable energy systems.



Ziping Wu was born in Tianjin, China, in 1982. He received the B.E degree in thermal power engineering and M.S degree in electrical power engineering from North China Electric Power University, Beijing, China, in 2006 and 2009, respectively. After graduation, he worked as an electrical engineer in China Electrical Power Research Institute from 2009 to 2011. His work mainly focused on the bulk power system modeling and simulation as well as HVDC transmission engineering. Since 2011, he has been pursuing the Ph.D. degree in the Department of Electrical and Computer Engineering, University of Denver. His current research interests include wind power generation, renewable energy, smart grid.



Eduard Muljadi (M'82, SM'94, F'10) received his Ph.D. in electrical engineering from the University of Wisconsin at Madison. From 1988 to 1992, he taught at California State University at Fresno. In June 1992, he joined the National Renewable Energy Laboratory in Golden, Colorado. His current research interests are in the fields of electric machines, power electronics, and power systems in general with an emphasis on renewable energy applications. He is member of Eta Kappa Nu and Sigma Xi, a fellow of the Institute of Electrical and Electronics Engineers (IEEE), and an editor of the *IEEE Transactions on Energy Conversion*. He is involved in the activities of the IEEE Industry Application Society (IAS), Power Electronics Society, and Power and Energy Society (PES). He is currently a member of various committees of the IAS, and a member of the Working Group on Renewable Technologies and the Task Force on Dynamic Performance of Wind Power Generation, both of the PES. He holds two patents in power conversion for renewable energy.



Wenzhong Gao (S'00–M'02–SM'03) received the M.S. and Ph.D. degrees in electrical and computer engineering specializing in electric power engineering from Georgia Institute of Technology, Atlanta, in 1999 and 2002, respectively. He is currently with the Department of Electrical and Computer Engineering, University of Denver, Colorado, USA. His current teaching and research interests include renewable energy and distributed generation, smart grid, power system protection, power electronics applications in power systems, power system modeling and simulation, and hybrid electric propulsion systems. He is an Editor for *IEEE Transactions on Sustainable Energy*. He is the General Chair for The IEEE Symposium on Power Electronics and Machines in Wind Applications (PEMWA 2012).